J|A|C|S
ARTICLES
Published on Web 09/05/2002

Stability, Metastability, and Unstability of Three-Electron-Bonded Radical Anions. A Model ab Initio Theoretical Study

Benoît Braïda,[†] Lea Thogersen,[†] Wei Wu,[‡] and Philippe C. Hiberty*[,†]

Contribution from the Laboratoire de Chimie Physique, Groupe de Chimie Théorique, Bat 490, Université de Paris-Sud, 91405 ORSAY Cédex, France, and Department of Chemistry and State Key Laboratory for Physical Chemistry of Solid Surfaces, Xiamen University, Xiamen, Fujian 361005, People's Republic of China

Received April 27, 2002

Abstract: The stability of O∴O, N∴N, S∴S, P∴P, and Si∴Si three-electron bonds in anionic radicals isoelectronic to dihalogen radical anions is studied by means of ab initio calculations on model systems. The difficulty of generating the dissociation energy profiles of such anions and their rearrangement to neutral species is solved by a practical method which consists of calculating the neutral and anionic energy profiles separately and shifting the curves with respect to each other to match the experimental energy gap between the asymptotes. Here the neutral and anionic reaction profiles are calculated at the CASPT2 and MP2 levels, respectively. The calculations predict that the O∴O bond is likely to be observed in anions of the type $[RO\therefore OR]^{\bullet -}$, where R is any alkyl substituent or carbon chain. The anion $Si_2H_6^{\bullet -}$ is found to be a metastable species, with a fair barrier to electron detachment. The barrier is much smaller for $N_2H_4^{\bullet -}$ and $P_2H_4^{\bullet -}$, thus precluding experimental observation. However, these species can be stabilized by electron-attractor substituents, the effect of which can be quantitatively estimated by means of the parent anion's diagrams and some fast complementary calculations. An example is given with the $[CF_3HN\therefore NHCF_3]^{\bullet -}$ anionic complex.

I. Introduction

Two-center three-electron (2c-3e) bonds can be encountered in many different areas such as free-radical chemistry,[1] biochemistry,[2] intrazeolite photochemistry,[3,4] and bioinorganic enzymology.[5,6] Three-electron bonds are preferentially observed in cations, but can also be detected in neutral[7−12] and anionic[8,10,13−20] adducts. Such molecules are held together by a three-electron interaction (noted ∴), also called a σ^* bond, in which one bonding σ molecular orbital (MO) is doubly occupied while the corresponding σ^* antibonding MO is singly occupied, leading to a net bond order of 0.5 and to a bonding energy on the order of 1 eV or more.

On the experimental side, all radical cation dimers of rare gases of the type $[Rg\therefore Rg]^{\bullet +}$ (Rg = He, Ne, Ar, etc.) are well

* To whom correspondence should be addressed. E-mail: philippe.hiberty@lcp.u-psud.fr.
[†] Université de Paris-Sud. The Laboratoire de Chimie Physique is associated with the CNRS, UMR 8000.
[‡] Xiamen University.

(1) For leading references, see: (a) Asmus, K. D. *Acc. Chem. Res.* **1979**, *12*, 436. (b) Göbl, M.; Bonifacic, M.; Asmus, K. D. *J. Am. Chem. Soc.* **1984**, *106*, 5984. (c) Asmus, K. D. *Nukleonika* **2000**, *45*, 3 and references therein.
(2) (a) Asmus, K.-D. In *Sulfur-Centered Reactive Intermediates in Chemistry and Biology*; Chatgilialoglu, C., Amus K.-D., Eds.; Plenum Press: New York and London, 1990; p 155.; (b) Glass, R. S. In *Sulfur-Centered Reactive Intermediates in Chemistry and Biology*; Chatgilialoglu, C., Amus K.-D., Eds.; Plenum Press: New York and London, 1990; p 213. (c) Gilbert, B. C. In *Sulfur-Centered Reactive Intermediates in Chemistry and Biology*; Chatgilialoglu, C., Amus K.-D., Eds.; Plenum Press: New York and London, 1990;p 135.
(3) Scaiano, J. C.; García, S.; García, H. *Tetrahedron Lett.* **1997**, *38*, 5929.
(4) Lakkaraju, P. S.; Shen, K.; Roth, H. D.; García, H. *J. Phys. Chem. A* **1999**, *103*, 7381.
(5) (a) Ortiz de Montellano, P. R. O. *Acc. Chem. Res.* **1987**, *20*, 289. (b) Sono, M.; Roach, M. P.; Coulter, E. D.; Dawson, J. H. *Chem. Rev.* **1996**, *96*, 2841 and references therein.
(6) (a) Shaik, S.; Filatov, M.; Schröder, D.; Schwarz, H. *Chem.—Eur. J.* **1998**, *4*, 193. (b) Ogliaro, F.; Harris, N.; Cohen, S.; Filatov, M.; De Visser, S. P.; Shaik, S. *J. Am. Chem. Soc.* **2000**, *122*, 8977 and references therein.
(7) Steffen, L. K.; Glass, R. S.; Sabahi, M.; Wilson, G. S.; Schöneich, C.; Mahling, S.; Asmus, K. D. *J. Am. Chem. Soc.* **1991**, *113*, 2141.
(8) Abu-Raqabah, A.; Symons, M. C. R. *J. Chem. Soc., Faraday Trans.* **1990**, *86*, 3293 and refs 4−7 therein.
(9) Abu-Raqabah, A.; Symons, M. C. R. *J. Am. Chem. Soc.* **1990**, *112*, 8614.
(10) Champagne, M. H.; Mullins, M. W.; Colson, A. O.; Sevilla, M. D. *J. Phys. Chem.* **1991**, *95*, 6487.
(11) (a) Janssen, R. A. J.; Aagaard, O. M.; Van der Woerd, M. J.; Buck, H. M. *Chem. Phys. Lett.* **1990**, *171*, 127. (b) Aagaard, O. M.; De Waal, B. F. M.; Cabbolet, M. J. T. F.; Janssen, R. A. J. *J. Phys. Chem.* **1992**, *96*, 614.
(12) Chateauneuf, J. E. *Chem. Commun.* **1998**, 2099.
(13) Wang, W.; Schuchmann, M. N.; Schuchmann, H. P.; Knolle, W.; Von Sonntag, J.; Von Sonntag, C. *J. Am. Chem. Soc.* **1999**, *121*, 238.
(14) El Hanine Lmoumène, C.; Conte, D.; Jacquot, J.-P.; Houée-Levin, C. *Biochemistry* **2000**, *39*, 9295.
(15) Abu-Raqabah, A.; Symons, M. C. R. *J. Chem. Soc., Faraday Trans.* **1990**, *86*, 3293 and refs 4−7 therein.
(16) Raynor, J. B.; Rowland, I. J.; Symons, M. C. R. *J. Chem. Soc., Faraday Trans.* **1991**, *87*, 571.
(17) (a) Bowman, R. J.; Symons, M. C. R. *J. Chem. Soc., Perkin Trans. 2* **1990**, 975. (b) Shanker Rai, U.; Symons, M. C. R.; Wyatt, J. L.; Bowman, R. *J. Chem. Soc., Faraday Trans.* **1993**, *89*, 1199.
(18) (a) Marignier, J.-L.; Belloni, J. *J. Phys. Chem.* **1981**, *85*, 3100. (b) Belloni, J.; Marignier, J.-L.; Katsumura, Y.; Tabata, Y. *J Phys. Chem.* **1986**, *90*, 4014. (c) Belloni, J.; Marignier, J.-L. *Radiat. Phys. Chem.* **1989**, *34*, 157. (d) Gauduel, Y.; Pommeret, S.; Antonetti, A.; Belloni, J.; Marignier, J.-L. *J. Phys.* **1991**, *1*, 161.
(19) (a) Berges, J.; Kassab, E.; Adjadj, E. Houée-Levin, C. *J. Phys. Chem.* **1997**, 101, 7809. (b) Berges, J.; Fuster, F.; Jacquot, J.-P.; Silvi, B.; Houée-Levin, C. *Nukleonika* **2000**, *45*, 2329.
(20) Gauduel, Y.; Marignier, J.-L.; Belloni, J.; Gelabert, H. *J. Phys. Chem. A* **1997**, *101*, 8979.

documented and their bonding energies accurately known, on the order of 25−30 kcal/mol (105−125 kJ/mol) or more.[21−23] Quite logically, their isoelectronic analogues of the type $[H_mX\therefore XH_n]^{\bullet+}$ have been shown, by means of ab initio calculations,[24,25] to be lower in energy than the dissociation products and to be stable except if they rearrange to even more stable hydrogen-bonded isomers. As for the radical anions, the series of halogen anionic dimers of the type $[X\therefore Y]^{\bullet-}$ (X, Y = F, Cl, Br, I, ...) is also well-known,[21,26−28] and one may wonder whether the organic isoelectronic species (e.g., $[RS\therefore SR]^{\bullet-}$, $[RO\therefore OR]^{\bullet-}$, etc.) display some significant stability. However, such anionic species have been the subject of much less numerous experimental or theoretical studies than three-electron-bonded cationic species, if one excepts the case of the hydrogen disulfide anion $[HS\therefore SH]^{\bullet-}$ and its substituted derivatives of biological interest.[29−35] Indeed, the disulfide linkage plays an important role in determining the biological activity of numerous proteins, enzymes, and antibiotics. The scission of the S−S bond in RS−SR molecules can occur through one-electron reduction, leading to a disulfide radical anion in equilibrium with the dissociated species. Radical anions of sulfur-containing compounds have been observed in the pulse radiolysis of cystine and cysteamine,[36] hydrogen sulfide, and mercaptans.[37,38] Thermal and photochemical studies indicate that the sulfhydril radical and its anion form the complex $H_2S_2^{\bullet-}$. Electron paramagnetic resonance (EPR) studies emphasize the formation of this species in glassy matrixes[34,39] and on magnesium oxide.[40] More generally, disulfide anions are involved in protection mechanisms for biological systems subject to ionizing radiations or other forms of free-radical damage.[41]

Apart from this well-documented type of anionic radical, a few other three-electron-bonded organic anions ($[F_3C\therefore SH]^{\bullet-}$, $[F_3C\therefore SCH_3]^{\bullet-}$) have also been suggested to be absolute minima or critical points on potential surfaces.[42] The radical anions $FCN^{\bullet-}$ and $FNC^{\bullet-}$ have been studied at high ab initio levels of theory by Sommerfeld,[43] and found to possess weak three-electron bonds. On the other hand, the three-electron-bonded conformation of the $H_2O_2^{\bullet-}$ radical anion has been shown to collapse, with an extremely small barrier, to two stable isomers which are best described as the electrostatic complexes $[HO^-\cdots HO^\bullet]$ and $[O^{\bullet-}\cdots HOH]$.[44−47] This instability of the three-electron-bonded conformation is due to the ease with which one of the hydrogens can flip to form a hydrogen bond with the oxygen atoms, which suggests that other species, of the type $[RO\therefore OR]^{\bullet-}$, might be stable.

The $P_2H_4^{\bullet-}$ and $N_2H_4^{\bullet-}$ systems have been studied by Simons et al.[48,49] at a rather high level of theory, CCSD(T) in large basis set including diffuse functions. $HPPH_3^{\bullet-}$ was found to exist as a dipole-supported state, but no valence state was found for the three-electron-bonded isomer $[H_2P\therefore PH_2]^{\bullet-}$.[48] Analogous conclusions were drawn from the study of $N_2H_4^{\bullet-}$.[49] On the other hand, the $[H_3Si\therefore SiH_3]^{\bullet-}$ complex has been found to be stable by Tada et al.,[50] at the MP2 level in a basis set involving diffuse orbitals with optimized exponents. At variance with the studies of Simons et al.,[48,49] a theoretical study of some radical anions of the type $[H_nX\therefore YH_m]^{\bullet-}$ (X, Y = Cl, S, P, Si, F, O, N, C; n, m = 0, 2) by Fourré et al.[51] has found some of these anions to be stable at the level of density functional theory (DFT), including $[H_3Si\therefore SiH_3]^{\bullet-}$, $[H_2P\therefore PH_2]^{\bullet-}$, and $[H_2N\therefore NH_2]^{\bullet-}$.

Such contrasting results illustrate the difficulties that are encountered in the theoretical studies of three-electron bonding in anions, among which are the (i) unstability of the energy with respect to inclusion of more and more diffuse functions in the basis set, (ii) adequacy of the orbitals arising from the orbital optimization step for further electron correlation treatment,[28] (iii) general overestimation of three-electron bonding energies by DFT methods,[52] and (iv) size of the energy barrier to electron detachment, which has been found by Sevin et al.[42] to be extremely basis set dependent. These theoretical difficulties are discussed in more detail in the next section, together with a proposed strategy to overcome them, by means of a method specifically relevant to the problem of three-electron bonding in radical anions.

The aim of this work is to apply the proposed method to study some model radical anions that are isoelectronic to dihalogen anions and possible candidates for stability, namely, $[H_3CO\therefore OCH_3]^{\bullet-}$, $[H_3Si\therefore SiH_3]^{\bullet-}$, $[H_2P\therefore PH_2]^{\bullet-}$, and $[H_2N\therefore NH_2]^{\bullet-}$ in addition to the well-known $[HS\therefore SH]^{\bullet-}$, and more generally to predict which types of radical-anion association have a chance to lead to stable or metastable species.

(21) See the compilation of experimental bonding energies in Gilbert, T. L.; Wahl, A. C. *J. Chem. Phys.* **1971**, *55*, 5247.
(22) Huber, K. P.; Herzberg, G. *Molecular Spectra and Molecular Structure IV. Constants of Diatomic Molecules*; Van Nostrand Reinhold: New York, 1979.
(23) Dehmer, P. H.; Pratt, S. T. In *Photophysics and Photochemistry in the Vacuum Ultraviolet*; McGlynn, S. P., Findley, G. L., Hueber, R. H., Eds.; D. Reidel Publishing Co.: Dordrecht, The Netherlands, 1985; p 260.
(24) Clark, T. *J. Am. Chem. Soc.* **1988**, *110*, 1672−1678
(25) Gill P. M. W.; Radom L. *J. Am. Chem. Soc.* **1988**, *110*, 4931−4941
(26) (a) Chen, E. C. M.; Wentworth, W. E. *J. Phys. Chem.* **1985**, *89*, 4099. (b) Dojahn, J. G.; Chen, E. C. M.; Wentworth, W. E. *J. Phys. Chem.* **1996**, *100*, 9649
(27) (a) Bowmaker, G. A.; Schmerdtfeger, P.; Von Szentpály, L. *J. Mol. Struct.: THEOCHEM* **1989**, 87. (b) Wenthold, P. G.; Squires, R. R. *J. Phys. Chem.* **1995**, *99*, 2002.
(28) Braïda, B.; Hiberty, P. C. *J. Phys. Chem. A* **2000**, *104*, 4618−4628
(29) Naito, A.; Akasaka, K.; Hatano, H. *J. Magn. Reson.* **1976**, *24*, 53.
(30) Bonnazola, L.; Michaut, J. P.; Roncin, J. *J. Chem. Phys.* **1985**, *83*, 2727.
(31) Colaneri, M. J.; Box, H. C. *J. Chem. Phys.* **1986**, *84*, 2926.
(32) Franzi, R.; Geoffroy, M.; Reddy, M. V. V. S.; Weber, J. *J. Phys. Chem.* **1987**, *91*, 3187.
(33) (a) Surdhar, P. S.; Armstrong, D. A. *J. Phys. Chem.* **1986**, *90*, 5915. (b) Surdhar, P. S.; Armstrong, D. A. *J. Phys. Chem.* **1987**, *91*, 6532.
(34) Zhu, J.; Petit, K.; Colson, A. O.; DeBolt, S.; Sevilla, M. D. *J. Phys. Chem.* **1991**, *95*, 3676.
(35) Benassi, R.; Taddei, F. *J. Phys. Chem. A* **1998**, *102*, 6173
(36) Mezyk, S. P. *Chem. Phys. Lett.* **1995**, *235*, 89.
(37) Karmann, W.; Meissner, G.; Henglein, A. *Z. Naturforsch.* **1967**, *B22*, 273.
(38) Karmann, W.; Granzow, A.; Meissner, G.; Henglein, A. *Int. J. Radiat. Phys. Chem.* **1969**, *1*, 395.
(39) Lin, M. J.; Lunsford, J. H. *J. Phys. Chem.* **1976**, *80*, 2015.
(40) Benassi, R.; Fiandri, G. L.; Taddei, F. *Tetrahedron* **1994**, *43*, 12469.
(41) (a) Schöneich, C.; Aced, A.; Asmus, K. D. *J. Am. Chem. Soc.* **1991**, *113*, 375. (b) Schöneich, C.; Aced, A.; Asmus, K. D. *J. Am. Chem. Soc.* **1993**, *115*, 11376. (c) Schöneich, C.; Bobrowski, K. *J. Phys. Chem.* **1994**, *98*, 12613. (d) Kishore, K.; Anklam, E.; Aced, A.; Asmus, K.-D. *J. Phys. Chem. A* **2000**, *104*, 9646.
(42) Dézarnaud-Dandine, C.; Sevin, A. *J. Am. Chem. Soc.* **1996**, *118*, 4427.
(43) Sommerfeld, T. *Phys. Chem. Chem. Phys.* **2001**, *3*, 2394.
(44) Schroder D.; Schalley C. A.; Goldberg N.; Hrusak J.; Schwarz H. *Chem.—Eur. J.* **1996**, *2*, 1235.
(45) van Doren, J. M.; Barlow, S. E.; DePuy, C. H.; Bierbaum, V. *J. Am. Chem. Soc.* **1987**, *109*, 4412.
(46) Humbel, S.; Demachy, I.; Hiberty, P. C. *Chem. Phys. Lett.* **1995**, *247*, 126.
(47) Hrusak, J.; Friedrichs, H.; Schwarz, H.; Razafinjanahary, H.; Chermette, H. *J. Phys. Chem.* **1996**, *100*, 100.
(48) Skurski, P.; Gutowski, M.; Simons, J. *J. Chem. Phys.* **1999**, *110*, 274.
(49) Skurski, P.; Gutowski, M.; Simons, J. *J. Phys. Chem. A* **1999**, *103*, 625.
(50) Tada, T.; Yoshimura, R. *J. Phys. Chem. A* **1993**, *97*, 1019.
(51) Fourré, I.; Silvi, B.; Sevin, A.; Chevreau, H. *J. Phys. Chem. A* **2002**, *106*, 2561.
(52) (a) Noodleman, L.; Post, D., Baerends, E. J. *J. Phys. Chem.* **1982**, *64*, 159. (b) Braïda, B.; Hiberty, P. C.; Savin, A. *J. Phys. Chem. A* **1998**, *102*, 7872. (c) Sodupe, M.; Bertran, J.; Rodriguez-Santiago, L.; Baerends, E. J. *J. Phys. Chem. A* **1999**, *103*, 166. (d) Chermette, H.; Ciofini, I.; Mariotti, F.; Daul, C. *J. Chem. Phys.* **2001**, *115*, 11068.

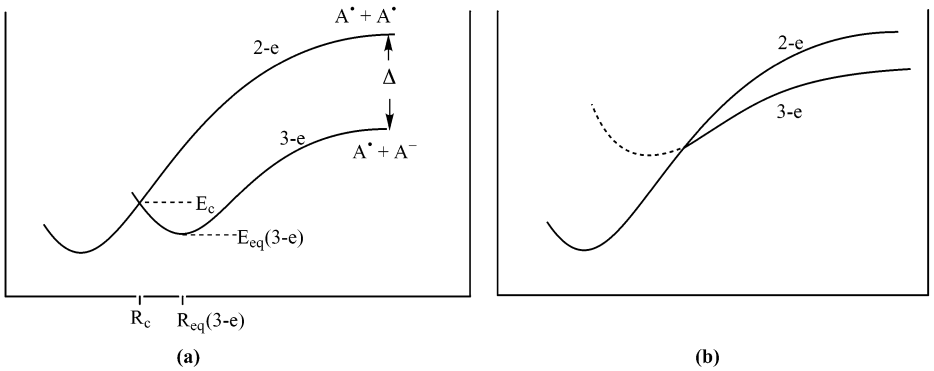

Figure 1. Schematic dissociation energy profiles for an A−A neutral molecule and its anion $[A\therefore A]^{\bullet -}$. R_{eq}(3-e) and E_{eq}(3-e) are the equilibrium distance and energy of the anion. Δ is the electron affinity of the A• radical. (a) Stable or metastable anion. (b) Unstable anion.

II. Qualitative Considerations and Computational Strategy

In the elementary approximation of molecular orbital theory, the formation of a three-electron bond between two equivalent fragments may be modeled by the perturbative interaction of the highest occupied molecular orbital (HOMO) of each fragment.[25] The interaction leads to a bonding σ MO which is doubly occupied, and to a singly occupied antibonding σ^* MO. Taking the initial energy of the fragment's HOMO as the origin (i.e., setting the traditional α parameter to zero in the extended Hückel model), one obtains the simplified diagram given below,

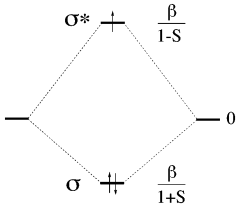

which shows that the three-electron bonding energy, D_e(3-e), is a simple function of S, the overlap between the two interacting fragment's orbitals, and β, the usual resonance integral in Hückel theory (eq 1).

$$D_e(3\text{-e}) = \beta(1 - 3S)/1 - S^2 \qquad (1)$$

Assuming that β is proportional to S, eq 1 shows that the three-electron interaction is always stabilizing at any interatomic distance such that the overlap S is smaller than 1/3, and simple differentiation shows that the bond gets its maximum strength for an optimal overlap value S_{opt} equal to 0.17. Now, since the interaction of an anion A^-, bearing a lone pair, with the corresponding radical A• is always stabilizing, why are some $A\therefore A^{\bullet -}$ radical anions stable (e.g., the dihalogen anions) while others are not (e.g., H_2^-)? The explanation is schematically illustrated in the two diagrams of Figure 1, which display some typical dissociation energy profiles for a neutral diatomic molecule A_2 and its anion.

In Figure 1a, bringing together a radical A and an anion A^- from infinite distance leads to a stabilizing interaction and to a local minimum at a distance R_{eq}(3-e). Further shortening the A−A distance makes the energy rise, until the anionic curve (3-e) crosses the dissociation energy curve of the neutral compound A_2 (2-e). At distances shorter than the crossing point, the electronic system gains some energy by expelling an electron or putting it in an infinitely diffuse orbital. This means that the part of the three-electron curve that is on the left-hand side of the crossing point (dotted line) is very much basis set dependent and, in fact, meaningless as far as bound states are concerned (we do not consider here temporary anions which display complex potential energy curves and cannot be studied with bound-state techniques[43]). Therefore, the height of the crossing point, relative to the three-electron interaction minimum, is a crucial quantity which determines the stability of the radical-anion adduct and its barrier $E^{\ddagger}$ to collapse to the neutral species.

Figure 1b describes another typical situation, where the minimum of the three-electron interaction can never be reached, because it is situated at distances shorter than the 2-e/3-e crossing point. This situation is typical of the H_2^- system. As one brings H^- and H• together, the energy goes down until the crossing point is reached, and then the electronic system expels an electron and collapses to the H_2 molecule. It is clear from Figure 1 that the energy gap Δ that separates the two asymptotes is a crucial parameter for the stability of the three-electron-bonded adduct. A large energy gap will lead to a diagram of type a, while small gaps are expected to correspond more likely to situation b. As this gap is nothing but the electron affinity (EA) of the neutral fragment A, there follows the general rule that a significant electron affinity of A is a factor that favors the stability of the $A\therefore A^{\bullet -}$ radical anion. This immediately explains why all dihalogen anions $X\therefore X^{\bullet -}$ are stable (EA(X) $\approx$ 3−4 eV typically) while H_2^- is not (EA(H) = 0.75 eV), and why three-electron bonds are preferentially observed in cations, for which the Δ gap is always large, being equal to the electron affinity of the cationic fragment.

From a theoretical point of view, the best way to estimate the stability of the $A\therefore A^{\bullet -}$ adduct is to generate the complete ground-state reaction profile, from the anionic system at long distance all the way to the minimum of the neutral A_2 species, which has expelled an electron. Doing this by a unique theoretical method requires a computational level that correctly places the 3-e curve relative to the 2-e one, i.e., a method that yields good electron affinities, a quantity that is particularly difficult to calculate in quantum chemistry (recall that DFT methods, which usually perform well for calculating EAs, are not adequate for describing three-electron bonds[52,53]). This

(53) (a) Merkle, F.; Savin, A.; Preuss, H. *J. Chem. Phys.* **1992**, *97*, 9216. (b) Bally, T.; Sastry, G. N. *J. Phys. Chem. A* **1997**, *101*, 7923. (c) Zhang, Y.; Yang, W. *J. Chem. Phys.* **1998**, *109*, 2604. (d) Chermette, H.; Ciofini, I.; Mariotti, F.; Daul, *J. Chem. Phys.* **2001**, *114*, 1447.

would necessitate the use of the very best treatments of electron correlation, together with very large basis sets involving high-rank polarization functions and flexible sets of diffuse functions. What we propose here is another strategy, based on the use of different methods to separately compute the 2-e and 3-e curves in the diagrams of Figure 1.

It is now well established[25,54,55] that the MP2 method provides reasonably accurate bonding energies for three-electron bonds, calculated as the difference between the energy of the equilibrium structure and the sum of the energies of the separate fragments. The reaction profile is also adequately calculated at this level, except at large interfragment distances where problems of symmetry-breaking inevitably occur.[55] However, we are not interested in this portion of the 3-e curve, since the crossing with the 2-e curve is expected to occur at rather short distances, and generally shorter than the equilibrium distance.

The MP2 method is therefore able to yield a realistic reaction profile in the interesting portion of the 3-e curve, as well as an asymptotic energy. On the other hand, the MP2 level is not adequate (see the Theoretical Section) for the 2-e reaction profile. For the best accuracy, this latter energy curve requires a CASPT2 calculation, including two configurations (the ground configuration and the lowest diexcited one) in the active space. Of course, these two separate calculations will not give us a correct energy spacing between the two asymptotes. To remedy this deficiency, the method we propose consists of simply shifting the 3-e curve relative to the 2-e one so the gap Δ between the asymptotes exactly matches the experimental affinity of the neutral fragment $A^{\bullet}$.

As a result, the proposed strategy is expected to yield two reasonably accurate energy profiles which are correctly spaced, in terms of relative energies, with respect to each other. As there would be no matrix element to couple the two curves in an exact calculation (since the two states do not have the same number of electrons), the crossing is not avoided and the barrier of the $A\therefore A^{\bullet-}$ state to collapse to the neutral state is given by the energy difference between E_c, the energy of the crossing point, and E_{eq}(3-e), the energy of the 3-e minimum:

$$E^{\ddagger} \approx E_c - E_{eq}(3\text{-e}) \qquad (2)$$

Two further points are noteworthy: (i) Equation 2 only expresses a near equality because the above strategy is strictly valid only for diatomics. If one deals with polyatomic molecules, the 3-e and 2-e states have different optimal geometries for the interatomic distance R, so the "crossing point" is not a real one since it does not correspond to a unique common conformation of the two states. There results a necessary correction for the barrier $E^{\ddagger}$, which is discussed in more detail below. (ii) It is necessary to check that the MP2-calculated points of the 3-e curve are not basis set dependent, especially in the vicinity of the 2-e curve. This may happen because the UHF step of the MP2 method greatly upshifts the 3-e curve relative to the 2-e one, and may tend to expel an electron that would normally be bound in an exact calculation, resulting in an overly diffuse highest occupied MO. Remedies for such situations exist and will be discussed later.

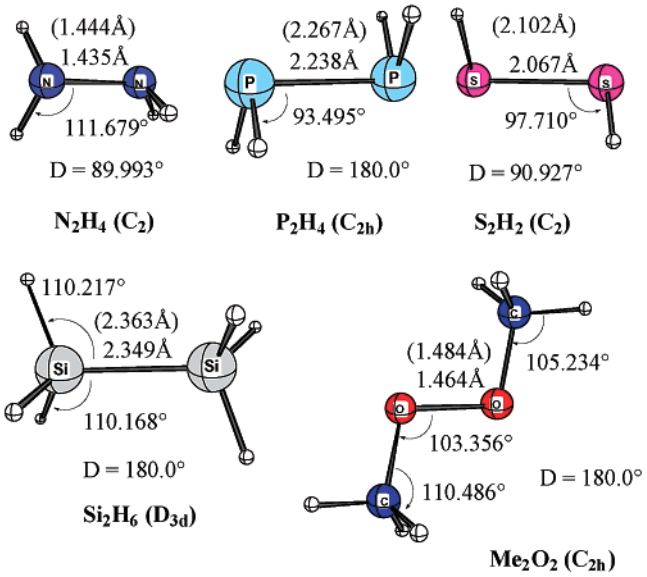

Figure 2. Some selected geometrical data for the H_nX-XH_n molecules, as optimized in the aug-cc-pVTZ basis set at the MP2 level. Bond lengths optimized in the aug-cc-pVDZ basis set are indicated in parentheses. D is the rotational angle about the X−X axis, with respect to a C_{2v} conformation.

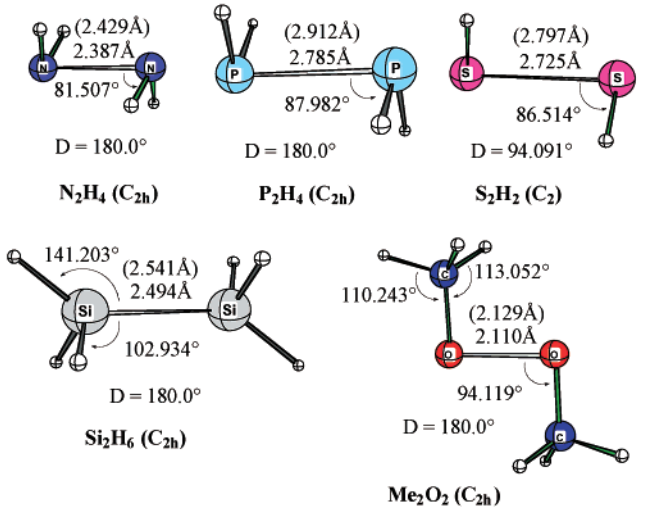

Figure 3. Same caption as Figure 2, for the $[H_nX\therefore XH_n]^{\bullet-}$ radical.

III. Theoretical Section

All the basis sets that have been used belong to the set of correlation-consistent basis sets of Dunning.[56] The standard double-ζ + polarization and triple-ζ + polarization basis sets are referred to as cc-pVDZ and cc-pVTZ, respectively. The aug-cc-pVDZ and aug-cc-pVTZ labels refer to the same basis set but augmented with s and p diffuse functions on all atoms except hydrogens. These latter basis sets are used for the optimization of the equilibrium geometries that are displayed in Figures 2 and 3, respectively, for the neutral compounds and for the anions. On the basis of test calculations which are described in the text, the calculations that have been made (geometry optimizations and single-point energies) to generate the dissociation curve of the neutral compounds have used the cc-pVTZ basis set, while similar calculations for the anionic curve

(54) Hiberty, P. C.; Humbel, S.; Danovich, D.; Shaik, S. *J. Am. Chem. Soc.* **1995**, *117*, 9003.
(55) Braïda, B.; Lauvergnat, D.; Hiberty, P. C. *J. Chem. Phys.* **2001**, *115*, 90.
(56) (a) Dunning, T. H., Jr. *J. Chem. Phys.* **1989**, *90*, 1007. (b) Kendall, R. A.; Dunning, T. H., Jr.; Harrison, J. *J. Chem. Phys.* **1992**, *96*, 6769. (c) Woon, D. E.; Dunning, T. H. *J. Chem. Phys.* **1993**, *98*, 1358.

have used the aug-cc-pVDZ basis set. Finally, an aug-cc-pVDZ basis set, further augmented with s and p Rydberg-type basis functions, of exponents 10 times smaller than the standard diffuse functions, has been used to check the basis set dependency of the MP2 calculations for the anions.

The Møller−Plesset many-body perturbation theory has been used to second order (MP2) in its spin-unrestricted form, for the optimization of equilibrium geometries for both neutral and anionic compounds (Figures 2 and 3). This latter method has also been used for generating the dissociation curves of the anions, referred to in the text as the 3-e curves. In each case, the 3-e curve is calculated only in the vicinity of its minimum, and the asymptotic energy is obtained as the sum of the energies of the separate fragments. Some test calculations have been done at the CCSD(T) level (coupled-cluster calculations including single and double excitations with a perturbative treatment of triples, using the MP2-optimized geometries) to ascertain the reliability of MP2 calculations for anions. On the other hand, the dissociation curves for the neutral compounds (2-e curves) were obtained using the CASPT2 method. This method consists, in the present case, of an MCSCF calculation that includes a two-electron, two-orbital (2,2) active space, followed by a second-order perturbation treatment of the Rayleigh−Schrödinger type. Note that the MP2 method would be inadequate for the 2-e curve, as soon as one would reach large interatomic distances where the low-lying diexcited configuration becomes important. On the other hand, a CASPT2 calculation would be meaningless for the 3-e curve, as there exists no low-lying excited configuration having the right symmetry to interact with the ground state. For each point of both the neutral and anionic dissociation curves, all geometrical parameters but the interfragment distance (R) are optimized, at the same computational levels as the single-point energy calculations. The experimental electron affinities that have been used to establish the energy gaps between the 3-e and 2-e asymptotes are from the site http:/webbook.nist.gov/chemistry, except for the EA of OCH_3, which was found in ref 57.

Some valence bond calculations have been done for the anions in cases where the MP2 method ceases to be valid, for reasons of basis set dependency. The "breathing orbital valence bond method" (BOVB)[58] has been used. This method optimizes the coefficients and orbitals of the VB structures simultaneously, with the specificity that the orbitals are allowed to be different for each VB structure. The method has been used in its simplest option, usually referred to as L-BOVB,[58d] in which all orbitals are defined as strictly localized on their respective fragment, i.e., one of the two fragments H_nX for an $[H_nX\therefore XH_n]^{\bullet-}$ anion.

The Gaussian 98 series of programs[59] has been used for all calculations of Møller−Plesset and coupled-cluster types. The MOLPRO package[60] has been used for the CASPT2 calculations. The valence bond calculations have been performed with the XIAMEN99 package.[61]

IV. Results and Discussion

Geometry Optimizations. The geometries or the neutral molecules and anions are shown in Figures 2 and 3, respectively, as optimized at the MP2 level. Two basis sets have been used, to check the basis set dependency. The geometrical parameters arising from the biggest basis set, aug-cc-pVTZ, are indicated in the figures. The values arising from the optimizations in the smallest basis set (aug-cc-pVDZ) are not indicated except for the equilibrium distance between the fragments, as this parameter is the only one that undergoes a significant difference from one basis set to the other.

According to the frequency calculations that have been performed in the smallest basis set, all stationary points shown in Figures 2 and 3 are true minima with only real frequencies. Perhaps surprisingly, all anionic complexes are stable at the MP2 level, and none of them collapse to a geometry close to that of the neutral fragment. The geometries of the neutral molecules are consistent with expectations based on standard bond lengths and bond angles, and do not display much basis set dependency. The largest deviations from one basis set to the other amount to only 0.4° for the angles and 0.035 Å for the bond lengths.

The geometries of the anions are more diversified. For $Me_2O_2^{\bullet-}$, $P_2H_4^{\bullet-}$, and $S_2H_2^{\bullet-}$, the bond angles are as expected, and such that the HOMO of one fragment points toward that of the other fragment, indicating an optimal three-electron interaction between these orbitals. The geometry of the N_2H_4 complex slightly departs from this idealized picture, with a rather small HNN angle, indicating some interaction of electrostatic type between the hydrogens of one fragment and the nitrogen atom of the other. For these four complexes, the interfragment distance is significantly elongated relative to that of the neutral compound, in harmony with the qualitative model above, which states that three-electron bonds prefer weak overlaps.

The case of $Si_2H_6^{\bullet-}$ is very particular. Its Si−Si bond length is not much longer than in the neutral molecule, and its geometry departs very much from the D_{3d} symmetry, so the HOMO of each SiH_3 fragment points to a direction that largely deviates from the Si−Si axis, showing that this anion exhibits a bonding scheme that is more complex than a simple three-electron bond.

The geometries of the anions are, in general, not more basis set dependent than those of the neutrals, with the notable exception of $P_2H_4^{\bullet-}$, in which the P−P bond length is almost 0.13 Å shorter in the largest basis set than in the other one.

(57) *CRC Handbook of Chemistry and Physics*, 70th ed.; CRC Press: Boca Raton, FL, 1989−1990; p E-67.
(58) (a) Hiberty, P. C.; Flament, J. P.; Noizet, E. *Chem. Phys. Lett.* **1992**, *189*, 259. (b) Hiberty, P. C.; Humbel, S.; Byrman, C. P.; van Lenthe, J. H. *J. Chem. Phys.* **1994**, *101*, 5969. (c) Hiberty, P. C.; Humbel, Archirel, P. *J. Phys. Chem.* **1994**, *98*, 11697. (d) Hiberty, P. C. In *Modern Electronic Structure Theory and Applications in Organic Chemistry*; Davidson, E. R., Ed.; World Scientific: River Edge, NY, 1997; pp 289−367.
(59) Frisch, M. J.; Trucks, G. W.; Schlegel, H. B.; Scuseria, G. E.; Robb, M. A.; Cheeseman, J. R.; Zakrzewski, V. G.; Montgomery, J. A., Jr.; Stratmann, R. E.; Burant, J. C.; Dapprich, S.; Millam, J. M.; Daniels, A. D.; Kudin, K. N.; Strain, M. C.; Farkas, O.; Tomasi, J.; Barone, V.; Cossi, M.; Cammi, R.; Mennucci, B.; Pomelli, C.; Adamo, C.; Clifford, S.; Ochterski, J.; Petersson, G. A.; Ayala, P. Y.; Cui, Q.; Morokuma, K.; Malick, D. K.; Rabuck, A. D.; Raghavachari, K.; Foresman, J. B.; Cioslowski, J.; Ortiz, J. V.; Stefanov, B. B.; Liu, G.; Liashenko, A.; Piskorz, P.; Komaromi, I.; Gomperts, R.; Martin, R. L.; Fox, D. J.; Keith, T.; Al-Laham, M. A.; Peng, C. Y.; Nanayakkara, A.; Gonzalez, C.; Challacombe, M.; Gill, P. M. W.; Johnson, B.; Chen, W.; Wong, M. W.; Andres, J. L.; Gonzalez, C.; Head-Gordon, M.; Replogle, E. S.; Pople, J. A. *Guassian 98* (revision A.6); Gaussian, Inc.: Pittsburgh, PA, 1998.
(60) MOLPRO is a package of ab initio programs written by H.-J. Werner and P. J. Knowles, with contributions from R. D. Amos, A. Bernhardsson, A. Berning, P. Celani, D. L. Cooper, M. J. O. Deegan, A. J. Dobbyn, F. Eckert, C. Hampel, G. Hetzer, T. Korona, R. Lindh, A. W. Lloyd, S. J. McNicholas, F. R. Manby, W. Meyer, M. E. Mura, A. Nicklass, P. Palmieri, R. Pitzer, G. Rauhut, M. Schütz, H. Stoll, A. J. Stone, R. Tarroni, and T. Thorsteinsson.
(61) Wu, W.; Song, L.; Mo, Y.; Zhang, Q. *XIAMEN99—An ab initio Spin-Free Valence Bond Program*; Xiamen University: Fujian, People's Repulic of China, 1999.

Table 1. Calculated Dissociation Energies, kcal/mol, for the Neutral Molecules and Their Three-Electron-Bonded Anions

	Neutral Species				
	N_2H_4	P_2H_4	Si_2H_6	O_2Me_2	S_2H_2
CASPT2/ccpVDZ	66.36	49.55	69.55	38.96	51.72
CASPT2/ccpVTZ	69.09	53.36	73.49	41.85	58.22
	Anionic Species				
	$N_2H_4^{\bullet-}$	$P_2H_4^{\bullet-}$	$Si_2H_6^{\bullet-}$	$O_2Me_2^{\bullet-}$	$S_2H_2^{\bullet-}$
MP2/aug-ccpVDZ	15.83	20.59	27.16	19.11	24.98
MP2/aug-ccpVTZ	15.83	22.49	30.28	18.87	26.86
CCSD(T)/aug-ccpVTZ	18.84	21.43	30.19		25.74

This change, however, is not as significant as it may appear, as the potential surfaces for the anions are particularly flat, as will be seen below.

Dissociation Energies. As the generation of the dissociation energy profiles for the neutral systems requires numerous geometry optimizations at the CASPT2 level, a choice has to be made for the basis set, combining efficiency and reasonable computational cost. Since diffuse functions are not really necessary for neutral species, the choice can be restricted to the cc-pVDZ basis set and the more flexible cc-pVTZ of triple-ζ quality, for this class of compounds. Table 1 displays the dissociation energies for the neutral compounds, as calculated at the CASPT2 level, in the two basis sets. Unlike the geometrical parameters (vide supra), the calculated values for the dissociation energies display some rather significant basis set dependency, being up to 5.5 kcal/mol larger in the largest basis set.

Diffuse functions are of course indispensable for the anions. Thus, the basis sets that are to be selected for this class of compounds must be of the "aug-cc-p" rather than simple "cc-p" type. Now, while the geometry optimizations proved, in one case ($P_2H_4^{\bullet-}$), rather sensitive to the choice of the basis set, it is interesting to also test the dissociation energies in this respect. Table 1 shows that the MP2-calculated dissociation energies display little basis set dependency, being about the same in the aug-cc-pVDZ and aug-cc-pVTZ basis sets. The adequacy of the MP2 level has also been checked by comparing MP2 and CCSD(T) values of the three-electron dissociation energies, as calculated in the aug-cc-pVTZ basis set. The agreement is generally good (see Table 1), with a maximum deviation of 3 kcal/mol for $N_2H_4^{\bullet-}$, too small to invalidate our MP2-based conclusions regarding the stability of this complex, as will be seen below.

The bonding energies of the anion complexes are sizable, on the order of 20−30 kcal/mol (84−125 kj/mol), and as such comparable to those of the three-electron-bonded radical cations.[24,25,52b] As in the latter systems, the bonding energies for the anions are found to increase as the central atoms are taken from left to right of the periodic table. Thus, recalling that F_2^- and Cl_2^- are bound by 30.2 and 31.8 kcal/mol experimentally,[26b] the bond strengths in the anions are in the following orders:

$$N\therefore N < O\therefore O < F\therefore F$$

$$P\therefore P < S\therefore S < Cl\therefore Cl$$

Interestingly, the methyl substituent is found to have a weakening effect on the O∴O bond. Indeed, the bonding energy of $Me_2O_2^{\bullet-}$ is only 18.8 kcal/mol, to be compared with the value 25.7 kcal/mol that has been calculated in a previous study for $H_2O_2^{\bullet-}$ in its metastable three-electron-bonded conformation.[46] This weakening effect of the methyl substituent is not a surprise, as it has already been shown to take place in radical cations for the N∴N, O∴O, and F∴F bonds.[62] Last, the Si∴Si bond is once again an exception in the above tendencies, being amazingly strong as compared to the P∴P bond. This is to be related to its peculiar geometry and exceptionally short interfragment distance.

2-e and 3-e Dissociation Energy Profile. Let us summarize the computational technique that has been devised to figure the 2-e and 3-e dissociation energy profiles on the same diagram. Each of the two curves is calculated by a method that is specific to it, CASPT2 for the 2-e curve and MP2 for the 3-e one. The two curves are also calculated in different basis sets. The curves are then shifted relative to each other so that the energy gap between the two asymptotes matches the experimental gap. The choice of the respective basis sets for the 2-e and 3-e curves has been made on the basis of the test calculations of geometries and dissociation energies above.

The computational tests that have been done above show that the dissociation energies are sensitive to the quality of the basis set for the neutral compounds. We have therefore selected the cc-pVTZ basis set for generating the 2-e energy profile. For the anionic species, the aug-cc-pVDZ basis set proved sufficiently accurate for the dissociation energies, and also for the geometries except in the $P_2H_4^{\bullet-}$ case. However, we will see below that this latter anion is the one that exhibits strong basis set dependency even in its equilibrium geometry, a sign that the MP2 method reaches its limit of validity for this species. In such a case, the triple-ζ basis set is in fact not better than the double-ζ one, as it is the computational method itself that becomes questionable. As will be seen later, the 3-e curve will be recalculated by another method (valence bond) for this molecule. In accord, the aug-cc-pVDZ basis set was seleted for generating the 3-e curves at the MP2 level.

The results are displayed in Figure 4. The points of the 3-e and 2-e curves are indicated by circles and squares, respectively. Let us disregard the triangles for the moment, as these points give the results of valence bond calculations that will be considered later.

a. $S_2H_2^{\bullet-}$. The dissociation curves for the S_2H_2 molecule and anion are shown in Figure 4a. It is immediately clear why the anionic complex is so readily observed: its minimum is situated largely below the 2-e minimum, so there exists no tendency to expel an electron to the continuum. In that respect, the situation for S_2H_2 is similar to that of the isoelectronic dihalogen molecules, which all have a large positive adiabatic electron affinity.

The shape of the left-hand side of the 3-e curve deserves comment. According to the qualitative model and to eq 1, this part of the curve should display a monotonic repulsive wall. By contrast, the curves exhibit a top and descend at short interatomic distances. This is the sign that the MP2 calculation ceases to be valid, and that the orbitals are probably spoiled with an excess of diffuse components. This point will be examined in detail in a further section.

(62) Braïda, B.; Hazebroucq, S.; Hiberty, P. C. *J. Am. Chem. Soc.* **2002**, *124*, 2371.

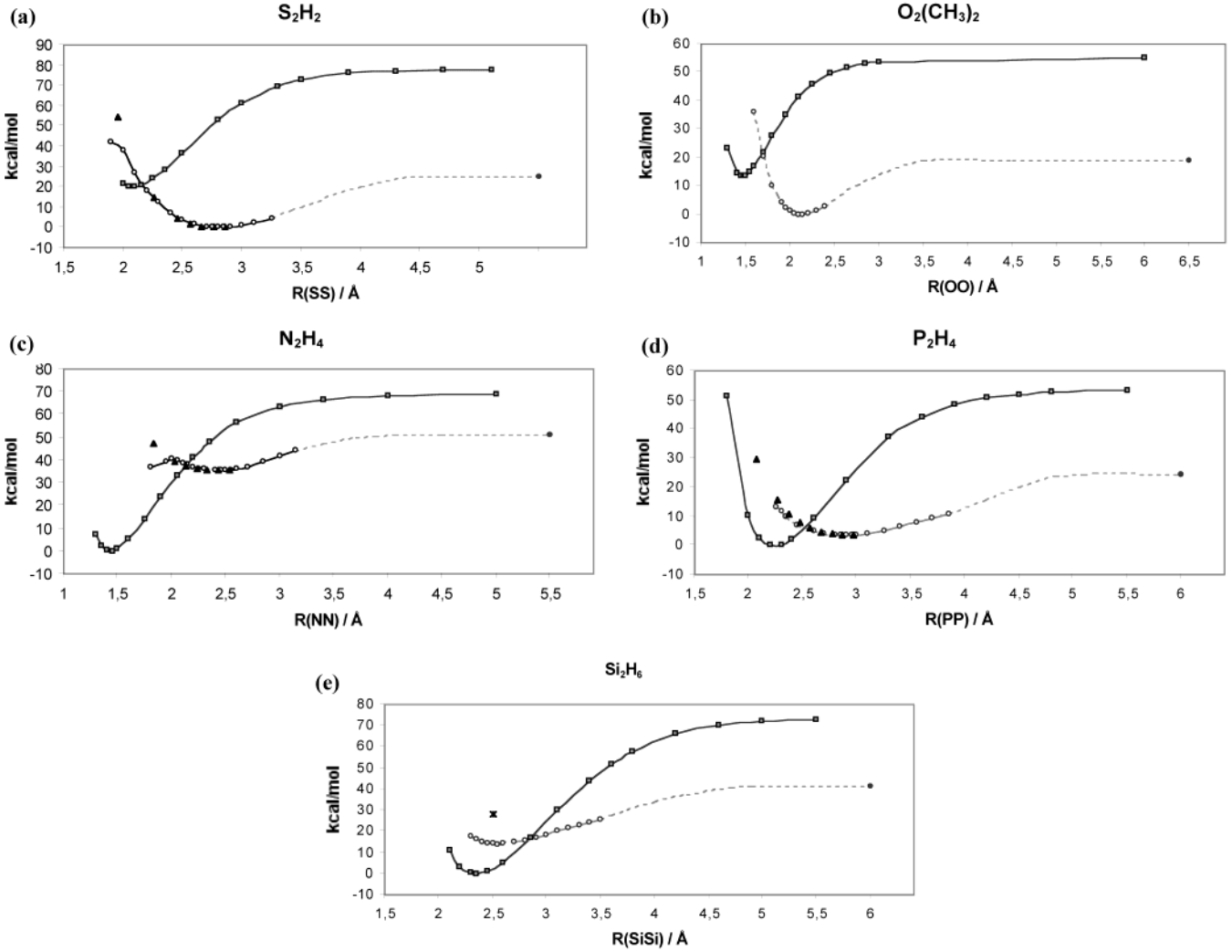

Figure 4. Calculated dissociation energy profiles for the H_nX-XH_n molecules and their anions. The experimental electron affinities that are used to construct the diagrams are as follows, in kcal/mol: 53.4 for $S_2H_2^{\bullet-}$, 36.2 for $O_2Me_2^{\bullet-}$, 29.3 for $P_2H_4^{\bullet-}$, 17.8 for $N_2H_4^{\bullet-}$, and 32.4 for $Si_2H_6^{\bullet-}$.

b. $Me_2O_2^{\bullet-}$. This complex is the methyl-substituted analogue of the $[HO\therefore OH]^{\bullet-}$ complex which has been studied by Humbel et al.[46] This latter anion has been found practically unstable in its three-electron-bonded conformation, not for lack of a strong interaction relative to the dissociated products, but because of a very facile rearrangement (**1** → **2** below) to a hydrogen-bonded

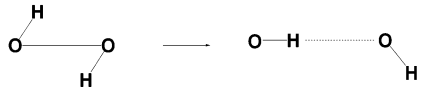

1 **2**

complex. As this rearrangement is linked to the very nature of the hydrogen atoms that are linked to the oxygens, the authors of this study concluded that a complex of the type $[RO\therefore OR]^{\bullet-}$ should be stable and observable. The present work indeed confirms this prediction, as the diagram for Me_2O_2 (Figure 4b) is qualitatively similar to the preceding one (Figure 4a), both showing an anionic complex lying below the neutral minimum.

c. $N_2H_4^{\bullet-}$ and $P_2H_4^{\bullet-}$. We now come to more delicate cases, those of the anions that have a bound valence state but are less stable than the optimized neutral + electron system. In each of these two cases, the 3-e minimum is situated on the right-hand side of the 3-e/2-e crossing point of the diagram (parts c and d, respectively, of Figure 4), and the corresponding difference of the abcissa is significant. Therefore, the two complexes are to be considered as theoretically stable, account not being taken of the zero-point vibration energy. However, owing to the flatness of the 3-e curves, the energy difference between the 3-e minimum and the crossing point is very low in both cases, on the order of 2−3 kcal/mol. While a more accurate estimation of the barrier to electron loss will be made in the next section, it is already apparent that these two anions exhibit too weak a metastability to be experimentally observable in the gas phase.

d. $Si_2H_6^{\bullet-}$. This case is different from the preceding ones in that the 3-e minimum is now situated on the *left-hand side* of the 3-e/2-e crossing point (Figure 4e). If this molecule were a diatomic, one would immediately conclude that the anion is unstable and spontaneously expels an electron. This would remain probable if the geometries of the neutral and anionic states were not too different for a given abcissa. However, as these two states display on the contrary very different bond angles, there is a chance that the energy of the neutral molecule, as calculated in the equilibrium geometry of the anion, is higher than the 3-e minimum, leading to a bound valence state for the anion. This has been checked, and the result is that Si_2H_6 is extremely destabilized, by 27.8 kcal/mol (at the CASPT2 level),

Table 2. Effect of Adding Rydberg Functions to the aug-cc-pVTZ Basis Set in the Single-Point Energy Calculations of the Anions[a]

	R_0	$R_0-0.1$	$R_0-0.2$	$R_0-0.3$	$R_0-0.4$	$R_0-0.5$	$R_0-0.6$
$HS\therefore SH^{\bullet-}$	0.024			0.046	0.17	0.55	7.2
	0.01			*0.02*	*0.04*	*1.65*	*16.0*
$MeO\therefore OMe^{\bullet-}$	0.082	0.098	0.125		0.272		
	0.03	*0.02*	*0.02*		*0.02*		
$H_3Si\therefore SiH_3^{\bullet-}$	0.013	0.058		0.285	0.548		
	0.006	*0.007*		*0.03*	*0.08*		
$H_2P\therefore PH_2^{\bullet-}$	0.718	1.414	8.76	9.27			
	0.17	*0.49*	*14.7*	*25.6*			
$H_2N\therefore NH_2^{\bullet-}$	0.121	0.175	0.275				
	0.18	*0.12*	*0.78*				

[a] For each entry, the numbers of the first line are the coefficients of the s Rydberg in the HOMO and are indicated as a function of the interatomic distance. The corresponding energy lowerings (ΔE(UHF)) are given as italic numbers, mhartrees. The distances are given in angstroms. R_0 is taken as the equilibrium distance in all cases except $Si_2H_6^{\bullet-}$, for which $R_0 = R_{eq} + 0.3$ Å.

when distorted from its equilibrium geometry to the anion's geometry. This destabilization, which is explained by the fact that the 2-e bond is practically broken in this geometry owing to the orientation of the methyl groups (see Figure 3), brings the vertical 2-e state 13.9 kcal/mol above the 3-e state (point shown as a star in Figure 4e). It follows that the $Si_2H_6^{\bullet-}$ complex is theoretically stable, in agreement with the study of Tada et al.,[50] and needs to distort up to the 3-e/2-e crossing point to achieve rearrangement to the 2-e state.

Validity of the 3-e Energy Profiles. While the validity of the CASPT2 calculations for the neutral species is beyond doubt, that of the MP2 calculations for the anions is a priori questionable. Indeed, the UHF step, which is used in the MP2 method to determine the orbitals, suffers from two well-known shortcomings: (i) it severely underestimates electron affinities, and (ii) it also greatly underestimates three-electron bonding energies.[54] This means that if the 2-e and 3-e curves were calculated at the UHF level, the 3-e curve would be greatly upshifted relative to the former. Of course, this defect is partly compensated by the fact that stretched geometries in the 2-e curve are also found too high relative to the 2-e minimum, but a danger remains that, for some geometries, the 3-e state displays an unbound electron at the UHF level, while this electron would be bound in an accurate calculation. When this happens, the consequence is that the HOMO of the anion involves an exceedingly large diffuse component, and becomes extremely basis set dependent: the more diffuse the functions added to the basis set, the lower the energy of the anions which would finally converge to the 2-e energy if an infinite basis set were used. In such a case, the MP2 calculation is of course invalid, and an easy test to detect the artifact consists of repeating the calculation in a basis set involving a very diffuse (Rydberg) function. Two factors are then examined: (i) the coefficient of the Rydberg function in the HOMO of the anion and (ii) the energy-lowering ΔE(UHF) that is found at the UHF level when Rydberg functions are added to the basis set.

This test has been done for all the points of the 3-e curve (see Table 2). Let us consider the case of $S_2H_2^{\bullet-}$ first, for which a large part of the MP2 curve is expected to be valid since it is much lower than the 2-e curve. Indeed, it can be seen in Table 2 that the coefficients of the Rydberg basis function remain marginal in the HOMO and lead to very small stabilizations for a large range of points around the equilibrium geometry. It is only for an S−S distance of 2.1 Å ($R_0 - 0.6$) that the Rydberg function begins to take an overwhelming importance, leading to an important stabilization at the UHF level (16.0 mhartrees). This critical distance closely corresponds to the 3-e/2-e crossing point. It is to be noted that, despite such warning signals, the MP2 3-e curve still seems to have a reasonable shape up to a distance of 1.9 Å, at which the curve starts to bend downward.

Quite like the preceding case, the MP2-calculated points for $Me_2O_2^{\bullet-}$ are stable with respect to an increase of the basis set, from the minimum to the region of the crossing point. The test is also satisfying for the $Si_2H_6^{\bullet-}$ anion, in agreement with our conclusions above and with the study of basis set effects by Tada et al.[50] On the other hand, difficulties are expected for $P_2H_4^{\bullet-}$ and $N_2H_4^{\bullet-}$, owing to the positions of their 3-e curves relative to the 2-e ones. Indeed, a significant contamination of the HOMO by the Rydberg function (with a coefficient of 0.7) is already observed at the 3-e equilibrium geometry of $P_2H_4^{\bullet-}$, and rapidly increases as the R distance is shortened. In the region of the crossing point, the Rydberg contribution is overwhelming. By contrast, the $N_2H_4^{\bullet-}$ anion appears as much less problematic than the preceding one, displaying little Rydberg contamination. Incidentally, this shows how difficult it is to make a priori predictions on such questions. Be it as it may, it is impossible to trust the MP2 results for the $P_2H_4^{\bullet-}$ energy profile, and the results are too inaccurate to allow any conclusions to be drawn on the stability of this anion. For a meaningful 3-e dissociation profile to be drawn in this case, a method other than MP2 must be used. As a necessary condition, the alternative method must well describe the three-electron interaction as early as the orbital-determining step. This latter requirement is well satisfied in the valence bond framework.

Valence Bond Calculations. The problem with the MP2 description of a three-electron-bonded anion is that the underlying UHF wave function (eq 3)

$$\Psi_{UHF}(3\text{-e}) = |...\sigma\bar{\sigma}\sigma^*| \qquad (3)$$

for the anion ressembles very much that of the neutral state. Indeed, if the σ^* orbital in eq 3 is infinitely diffuse, the UHF function figures nothing but a neutral state and an infinitely distant electron. Thus, the UHF wave function may represent, in fact, all kinds of pseudostates that are intermediates between the neutral molecule and the anion, according to the more or less diffuse character of σ^*, hence the possible Rydberg contamination and/or basis set dependency.

The situation is entirely different if a valence bond (VB) method is employed.[63] The VB wave function for the neutral state is expressed in eq 4

$$\Psi_{VB}(2\text{-e}) = |...\varphi_a\bar{\varphi}_b| + |...\varphi_b\bar{\varphi}_a| \qquad (4)$$

(dropping normalization factors), in which φ_a and φ_b are the atomic orbitals that are involved in the bond (and whose bonding combination is the σ MO). As for the anionic state, it is expressed by a wave function (eq 5)

$$\Psi_{VB}(3\text{-e}) = |...\varphi_a\bar{\varphi}_a\varphi_b| + |...\varphi_a\bar{\varphi}_b\varphi_b| \qquad (5)$$

that has little in common with the preceding one (eq 4). More

(63) The Hartree−Fock and VB descriptions of three-electron bonds are equivalent only in the minimal basis set, i.e., if no orbital optimization is performed (see ref 54).

specifically, eqs 4 and 5 show that there is no way for the 3-e state to collapse to the 2-e one by exceedingly increasing the diffuse character of any of its orbitals. It follows that the valence bond description of the 3-e state is stable with respect to a basis set increase, and that it is able to provide a wave function for a pure 3-e state even in geometries (very short distances) where the latter state is only virtual, the neutral state being the most stable one. Among the various computational methods of the VB type, we have chosen the BOVB method,[58] which is known to provide reliable bonding energies and dissociation energy profiles (see the Theoretical Section). The results are displayed in Figure 4a,c,d as filled triangles. To better compare the BOVB and MP2 reaction profiles, the BOVB curve has been shifted, in each case, so its minimum exactly coincides with the MP2 minimum.

Let us comment on the $S_2H_2^{\bullet-}$ case first (Figure 4a). It is seen that, from the 3-e minimum to the crossing point and even at shorter distances, the BOVB and MP2 curves are practically undistinguishable. It is only for an interatomic distance of nearly 1.9−2.0 Å that the two curves separate. As expected from the qualitative considerations above, the BOVB curve keeps generating a smooth repulsive wall while the MP2 curve falls and becomes meaningless. Incidentally, this test case also shows that the reaction profile displayed by the BOVB method is extremely close to the MP2 one in the regions where the latter method is valid.

The valence bond test has been repeated for the $N_2H_4^{\bullet-}$ and $P_2H_4^{\bullet-}$ anions (Figure 4c,d). In the $N_2H_4^{\bullet-}$ case, the BOVB curve merges into the MP2 one, which is not surprising since this anion is not subject to contamination by the Rydberg basis functions. In the $P_2H_4^{\bullet-}$ case, the MP2 and BOVB curves gradually separate, but to a small extent and only at distances distinctly on the left-hand side of the crossing point. It follows that the MP2 curves can be considered as reliable for each of the anions that have been studied here, in the range of interatomic distance that lies between the 3-e minimum and the 3-e/2-e crossing points, and can therefore serve as a basis to calculate the barriers to electron detachment.

Barriers to 3-e → 2-e Transitions. The "crossing points" that are seen in Figure 4 are not real ones, in that they correspond, for the same interatomic distance R_c, to different optimized geometries for the 3-e and 2-e states. Therefore, such points cannot correspond to an electronic transition between the two curves, and they yield nothing but lower limits for the barrier to electron expelling. To correct for this deficiency of the model, one may calculate, at the distance R_c, E_1, the energy of the anion in the geometry of the neutral, and E_2, the energy of the neutral in the geometry of the anion. The lowest of these energies, say E_1, is the energy of a possible geometry for the 3-e → 2-e transition, but not necessarily the best one. Thus, the energy range from E_c to E_1 provides an error bar for the barrier to the transition.

Calculations of E_1 and E_2 values have been made for the five anions under study. In all cases, the anion, as calculated in the neutral's geometry, is more stable than the reverse; i.e., E_1 is always lower than E_2. The barrier to the 3-e → 2-e transition was then estimated, with its error barr, through the following inequality:

$$E_c - E_{eq}(3\text{-e}) < \Delta E^{\ddagger} < E_1 - E_{eq}(3\text{-e}) \qquad (6)$$

Table 3. Lower and Higher Limits for the Barriers to Transition from the 3-e Curves to the 2-e Ones in Figure 4e[a]

	E_c[b]	E_1[c]		E_c[b]	E_1[c]
$N_2H_4^{\bullet-}$	2.74	2.98	$O_2Me_2^{\bullet-}$	22.61	25.33
$P_2H_4^{\bullet-}$	3.32	3.44	$S_2H_2^{\bullet-}$	20.87	22.44
$Si_2H_6^{\bullet-}$	2.0	10.38			

[a] All energies in kilocalories per mole, relative to the energy of the 3-e minimum. [b] Energy of the crossing point. [c] Energy of the anion in the optimized geometry of the neutral, at the abcissa of the crossing point.

The results, displayed in Table 3, show that the $E_1 - E_c$ error bar is very small for $N_2H_4^{\bullet-}$ and $P_2H_4^{\bullet-}$ (on the order of 1 kcal/mol), a little higher (2−3 kcal/mol) for $S_2H_2^{\bullet-}$ and $O_2Me_2^{\bullet-}$, and quite significant in the case of $Si_2H_6^{\bullet-}$, which is in line with the fact that the 3-e and 2-e geometries are very different from each other for this molecule (vide supra). It follows that this latter anion must undergo a relatively costly geometrical distortion to be able to expel an electron. The barrier to transition to the neutral state is not known with certainty from our calculations, being between 2.0 and 10.4 kcal/mol according to Table 3. To better estimate the barrier, one may in this case also consider the energy E_2, i.e., the energy of the neutral in the anion's geometry. It happens that E_2 is higher than E_1 by as much as 17.1 kcal/mol, indicating that the geometry for the real crossing point is probably much closer to the neutral's than to the anion's geometry. Therefore, it is probable that the energy of the real crossing point is not far from the E_1 limit, so the barrier to transition to the neutral state should not be much smaller than ∼10 kcal/mol (42 kJ/mol). A more accurate estimation would require a complete study of the crossing between the multidimensional 3-e and 2-e potential surfaces, which is beyond the scope of this study.

The present results lead to the following conclusions. Apart from the stability of $S_2H_2^{\bullet-}$, which is no surprise, the stability of the $[MeO\therefore OMe]^{\bullet-}$ anion is also clearly demonstrated. This compound is a generic model for many other anions involving an O∴O bond, such as alkyl-substituted compounds, carbon chains, rings, etc. All these three-electron-bonded anions should be stable and experimentally observable, as well as many differently substituted species. The anion $Si_2H_6^{\bullet-}$ is less stable than the corresponding neutral molecule. Nevertheless, it has a bound valence state and displays a barrier to electron expelling that we predict to be close to 10 kcal/mol. It is therefore a metastable compound that we tentatively predict to be experimentally observable at low temperatures. Moreover, as the isoelectronic systems $SiGeH_6^{\bullet-}$ and $Ge_2H_6^{\bullet-}$, which have been studied by Tada et al.,[50] exhibit similar characteristics, our predictions extend to these two further anions. On the other hand, the two remaining anions that have been studied in this work, $N_2H_4^{\bullet-}$ and $P_2H_4^{\bullet-}$, display a very shallow local minimum. Even without the ZPE corrections being estimated (which are anyway very small owing to the flatness of the potential surfaces), the barriers that separate the three-electron-bonded minima from the neutral states are in all cases very small, nearly 2−3 kcal/mol, leading to the firm conclusion that none of these anions can be experimentally observed in their three-electron-bonded conformations, at least in the gas phase. This of course does not deny the existence of other conformations for the $N_2H_4^{\bullet-}$ and $P_2H_4^{\bullet-}$ anions, such as the dipole-supported states that have been found by Simons et al.[48,49] Here our method is limited to three-electron-bonded structures, and

Table 4. Optimized Parameters for the $CF_3HN-NHCF_3$ Molecule and Its Anion[a]·Energies in Kcal/Mol, Distances in Å

	R_{eq}	D_e[c]	asymptote[b]
neutral[c]	1.408	81.0	59.98
anion[c]	2.276	25.4	0

[a] Energies in kilocalories per mole, distances in angstroms. [b] Taken as the electron affinity of the $NHCF_3$ fragment, as calculated at the CCSD(T) level. [c] Calculated at the MP2 level.

the possible rearrangements of such conformations to other isomers is the object of standard conformational studies, which pass the scope of the present work.

V. General Predictions for Other Anionic Systems

Let us consider diagrams c and d in Figure 4, which are typical of metastable three-electron-bonded anions ($N_2H_4^{\bullet-}$ and $P_2H_4^{\bullet-}$). Is it possible to make related systems observable, by appropriate substituent effects that would downshift the 3-e curve relative to the 2-e one? If the substituent effects are such that the 3-e minimum comes lower than the 2-e one, the three-electron-bonded anion is obviously stable. If not, one may wonder if a metastable anionic species, having a bound valence state albeit less stable than the neutral molecule, might be observable. In view of the shapes of the diagrams, this seems to be possible in the case of the N∴N bond, but very unlikely in the P∴P case because of the flatness of the 3-e curve and the small *R* distance that separates the 3-e minimum from the 2-e one. Be it as it may, it is not difficult to make predictions by starting from a model diagram such as c or d and shifting the 3-e vs 2-e curves according to the effects of substituents on the energy gap between the asymptotes. As this gap is nothing but the electron affinity of one of the separate fragments, electron-acceptor substituents have the effect of downshifting the 3-e curve relative to the 2-e curve, while donors have the reverse effect. An example is given below.

The CF_3 fragment is a well-known attractor substituent. In accord, the $[CF_3HN\therefore NHCF_3]^{\bullet-}$ can be expected to be stable and observable in its three-electron-bonded conformation **3**.

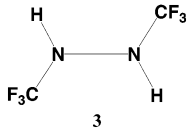

3

The calculations that are necessary to check this proposal are simple. We need the dissociation energy D_e(2-e) of the neutral molecule and that of the anion, D_e(3-e), and the electron affinity EA of the HCF_3N fragment. The stability ΔE(3-e) of the anionic fragment relative to the neutral one is given by eq 7.

$$\Delta E(\text{3-e}) = D_e(\text{2-e}) - D_e(\text{3-e}) - \text{EA}(HCF_3N) \qquad (7)$$

The calculations have been made in the aug-cc-pVTZ basis set and are displayed in Table 4. The neutral molecule and the anion have been studied at the MP2 level. For lack of an experimental electron affinity for the HCF_3N fragment, we calculated this value at the CCSD(T) level.

Let us first note that the equilibrium geometries for the 2-e and 3-e minima are separated by a distance of 0.87 Å on the reaction coordinate, which is not much different from the value 0.94 Å in $[H_2N\therefore NH_2]^{\bullet-}$, showing that the main characteristics of the diagrams of Figure 4, for the parent compounds, carry over to substituted species. The table also shows that the quantity ΔE(3-e) of eq 7 is found to be *negative*, − 4.2 kcal/mol, showing that the $[CF_3HN\therefore NHCF_3]^{\bullet-}$ anion is definitely stable. Many other electron-attractor substituents can be envisaged to stabilize an N∴N three-electron bond in an anionic radical.

VI. Conclusion

It is difficult to study the reaction profile of a three-electron-bonded anion along its dissociation coordinate by a single computational method. Unless the method is very sophisticated and uses very flexible basis sets, the region of the transition from the 3-e to the 2-e surface has all chances to be poorly described and to be possibly subject to artifacts and/or basis set dependency. We propose an alternative practical method, in which each of the 2-e and 3-e energy profiles is calculated by a method that is specific to it, and the curves are shifted with respect to each other to match the experimental energy gap between the asymptotes. In the present work, the CASPT2 has been selected to generate the 2-e reaction profile, and the MP2 method proved satisfactory for the 3-e curve, at least in the regions of interest.

The method is applied to a series of model systems which are isoelectronic to dihalogen anions and display a spectrum of three-electron bonds: O∴O, N∴N, S∴S, P∴P, and Si∴Si. The three-electron-bonded anions prove to share some common properties with their cationic analogues: the same orders of magnitude for the dissociation energies with respect to dissociated fragments and the same tendencies in the periodic table.

Some crucial points to estimate the stability or metastability of such ionic complexes are the energy of the anionic minimum relative to the neutral one and the barrier to transition from the anionic curve to the neutral one. Our results predict that the O∴O bond is likely to be observed in anions of the type $[RO\therefore OR]^{\bullet-}$, where R is any alkyl substituent or carbon chain. On the other hand, the anion $Si_2H_6^{\bullet-}$ is a metastable species that owes its stability, with respect to electron expelling, to the fact that the geometry of the anion is very different from that of the neutral state, in terms of bond angles. Last, $N_2H_4^{\bullet-}$ and $P_2H_4^{\bullet-}$ are both found to exhibit a bound valence state, however with an extremely small barrier to electron expelling by a transition from the 3-e curve to the 2-e one. These anions therefore cannot be experimentally observed in their three-electron-bonded conformations, at least in the gas phase or a matrix. However, appropriate substituent effects, by means of electron-attractor substituents, are expected to stabilize these species, as has been demonstrated in the case of $[CF_3HN\therefore NHCF_3]^{\bullet-}$. More generally, the calculations that are presented here can be used to predict substituent effects and the stability of substituted anions involving O∴O, N∴N, or P∴P bonds, by means of a a few calculated or experimentally known quantities such as dissociation energies and fragment electron affinities.

The present study suggests that many anionic radicals might be stable or metastable in their three-electron-bonded conformations, especially if they bear electron-attractor substituents. In view of their importance in biochemistry, it is hoped that the present work will stimulate further experimental research aiming at the experimental observation of novel three-electron-bonded anions.

JA026707Y